THE JOURNAL OF BIOLOGICAL CHEMISTRY Vol. 276, No. 3, Issue of January 19, pp. 2023–2030, 2001
Printed in U.S.A.

The Potency and Specificity of the Interaction between the IA_3 Inhibitor and Its Target Aspartic Proteinase from *Saccharomyces cerevisiae**

Received for publication, September 18, 2000, and in revised form, October 6, 2000
Published, JBC Papers in Press, October 19, 2000, DOI 10.1074/jbc.M008520200

Lowri H. Phylip,[a] Wendy E. Lees,[a,b] Brian G. Brownsey,[c] Daniel Bur,[d] Ben M. Dunn,[e] Jakob R. Winther,[f] Alla Gustchina,[g] Mi Li,[g,h] Terry Copeland,[i] Alexander Wlodawer,[g] and John Kay[a,j]

From the [a]School of Biosciences, Cardiff University, P. O. Box 911, Cardiff CF10 3US, Wales, United Kingdom, the [c]Department of Medicine, University of Wales College of Medicine, Cardiff CF14 4XN, Wales, United Kingdom, [d]F. Hoffmann La Roche AG, CH-4070 Basel, Switzerland, the [e]Department of Biochemistry & Molecular Biology, University of Florida College of Medicine, Gainesville, Florida 32610, the [f]Department of Yeast Genetics, Carlsberg Laboratory, DK-2500, Copenhagen Valby, Denmark, the [g]Protein Structure Section, Macromolecular Crystallography Laboratory, National Cancer Institute, Frederick, Maryland 21702, the [h]Intramural Research Support Program, SAIC Frederick, National Cancer Institute, Frederick, Maryland 21702, and the [i]Program Core, DBS, National Cancer Institute, Frederick, Maryland 21702

The yeast IA_3 polypeptide consists of only 68 residues, and the free inhibitor has little intrinsic secondary structure. IA_3 showed subnanomolar potency toward its target, proteinase A from *Saccharomyces cerevisiae*, and did not inhibit any of a large number of aspartic proteinases with similar sequences/structures from a wide variety of other species. Systematic truncation and mutagenesis of the IA_3 polypeptide revealed that the inhibitory activity is located in the N-terminal half of the sequence. Crystal structures of different forms of IA_3 complexed with proteinase A showed that residues in the N-terminal half of the IA_3 sequence became ordered and formed an almost perfect α-helix in the active site of the enzyme. This potent, specific interaction was directed primarily by hydrophobic interactions made by three key features in the inhibitory sequence. Whereas IA_3 was cut as a substrate by the nontarget aspartic proteinases, it was not cleaved by proteinase A. The random coil IA_3 polypeptide escapes cleavage by being stabilized in a helical conformation upon interaction with the active site of proteinase A. This results, paradoxically, in potent selective inhibition of the target enzyme.

Aspartic proteinases participate in a variety of physiological processes, and the onset of pathological conditions such as hypertension, gastric ulcers, and neoplastic diseases may be related to changes in the levels of their activity. Members of this proteinase family, *e.g.* renin, pepsin, cathepsin D, and human immunodeficiency virus-proteinase are generally typecast on the basis of their susceptibility to inhibition by naturally occurring, small molecule inhibitors such as the acylated pentapeptides, isovaleryl- and acetyl-pepstatin. However, the two most recently identified human aspartic proteinases, β-site Alzheimer's precursor protein cleavage enzyme and β-site Alzheimer's precursor protein cleavage enzyme 2 (1, 2), are not inhibited by this classical type of inhibitor of this family of enzymes. Pepstatins are metabolic products produced by various species of actinomycetes and, as such, are not themselves gene-encoded. Protein inhibitors of aspartic proteinases are relatively uncommon and are found in only a few specialized locations (3). Examples include renin-binding protein in mammalian kidneys which intriguingly has now itself been identified to be the enzyme, *N*-acetyl-D-glucosamine-2-epimerase (4); a 17-kDa inhibitor of pepsin and cathepsin E from the parasite, *Ascaris lumbricoides* (5); proteins from plants such as potato, tomato, and squash (6, 7), and a pluripotent inhibitor from sea anemone of cysteine proteinases as well as cathepsin D (8).

The IA_3 polypeptide in yeast is an 8-kDa inhibitor of the vacuolar aspartic proteinase (proteinase A or saccharopepsin) that was initially described by Holzer and co-workers (9). The complete sequence of this 68-residue inhibitor has been elucidated (10, 11) and the inhibitory activity of IA_3 has been shown to reside within the N-terminal half of the molecule (10, 12). We have recently solved the structure of the IA_3-proteinase A complex (12), demonstrating that whereas free IA_3 has little intrinsic secondary structure, residues 2–32 of the inhibitor, upon contact with proteinase A, become ordered and adopt a near perfect α-helical conformation occupying the active site cleft of the enzyme. This was the first crystal structure to be determined for a gene-encoded aspartic proteinase inhibitor complexed with its target enzyme. It was thus considered important to investigate further the role of the proteinase as a folding template and to attempt to establish the molecular features that enable this unprecedented mode of inhibitor-proteinase interaction to occur.

EXPERIMENTAL PROCEDURES

Protein Production and Purification—Proteinase A and other aspartic proteinases were obtained, and peptides were synthesized by solid-phase methods, as described previously (12). Genomic DNA was extracted from *S. cerevisiae* and the gene encoding IA3 was amplified specifically by polymerase chain reaction (PCR)[1] using 5′-GCATATG-

* This work was supported in part by a grant from the BBSRC, UK (to J. K.). The costs of publication of this article were defrayed in part by the payment of page charges. This article must therefore be hereby marked "*advertisement*" in accordance with 18 U.S.C. Section 1734 solely to indicate this fact.

The atomic coordinates and structure factors (code 1g0v) have been deposited in the Protein Data Bank, Research Collaboratory for Structural Bioinformatics, Rutgers University, New Brunswick, NJ (http://www.rcsb.org/).

[b] Supported by an award from Actelion, Allschwil, Switzerland.

[j] To whom correspondence should be addressed. Tel.: 44-29-20-87-41-24; Fax: 44-29-20-87-4116; E-mail: KayJ@Cardiff.ac.uk.

[1] The abbreviations used are: PCR, polymerase chain reaction; ACTH, adrenocorticotropic hormone; MALDI-TOF, matrix-assisted laser desorption-time of flight; MES, 4-morpholineethanesulfonic acid.

AATACAGACCAACAAAAAGTG-3′ and 5′-GCTCGAGCTCCTTCTTATGCCCCGC-3′ as forward and reverse primers. Mutations were introduced into the wild type sequence to generate clones encoding the chimera, $(Gly)_9$ and K7M proteins (Table I) by using the respective forward primers: chimera, 5′-GGAGATATACATATGGGAGGACACGACGTCCCTTTAACAAACATATTTCAGAGCTCA-3′; $(Gly)_9$, 5′-GCATATGGGAGGAGGCGGCGGCGGTGGAGGAGGCATATTTCAGAGCTCA-3′; and K7M, 5′-GCATATGAATACAGACCAACAAATGGTGAGCGAA-3′ in conjunction with the wild type reverse primer described above. The constructs encoding the K24M, K31M/K32M, Mix, D22L, and K18M/D22L mutants were each generated in two steps by overlapping PCR mutagenesis (13) using the mutagenic primer sets: K24M, forward, 5′-GGCGATGCAATGGTAGTGAGTGACGCTTTT-3′ and reverse, 5′-ACTCACTACCATTGCATCGCCCTGCAATTT-3′; K31M/K32M: forward, 5′-TTTATGATGATGGCCAGTCAAGACAAGGACGGC-3′ and reverse 5′-ACTGGCCATCATCATAAAAGCGTCACTCACTACCTT-3′; Mix: forward, 5′-AAGGCCGATAAATTTTCAATGGCTAGTCAAGACAAGG-3′ and reverse, 5′-TGAAAATTTATCGGCCTTCACTACCTTTGCATCGCC-3′; D22L: forward, 5′-CAGGGGCTGGCCAAGGTAGTGAGTGACGCTTTT-3′ and reverse, 5′-TACCTTGGCCAGCCCCTGCAACTTTTCCTTTGA-3′; K18M/D22L: forward, 5′-GAAATGTTGCAGGGGCTGGCCAAGGTAGTGAGTGACGCTTTT-3′ and reverse, 5′-ATCCTTGGCCAGCCCCTGCAACATTTCCTTTGAGCTCTGAAA-3′. The second set of overlap primers utilized the T7 forward primer and the wild type reverse primer described above.

Wild type and mutant forms of IA3 were subcloned into the *Nde*I-*Xho*I sites of pET-22b (Novagen, Cambridge, United Kingdom), thus introducing a C-terminal Leu-Glu-His_6 tag. *Escherichia coli* strain BL21DE3(pLysS) was transformed with wild type or mutant clones, then grown at 37 °C in LB medium to an A_{600} of ~0.6 before induction with 1 mM isopropyl-1-thio-β-D-galactopyranoside. Each soluble recombinant protein was loaded onto a nickel-chelate affinity column in 0.05 M sodium phosphate buffer, pH 8.0, containing 0.3 M NaCl, washed with the same buffer adjusted to pH 6.0 containing 10% glycerol and each protein form of IA_3 was eluted with the glycerol containing buffer at pH 4.0. Appropriate fractions containing IA_3 were then heated twice at 100 °C for 5 min.

Analytical Measurements—N-terminal sequencing of wild-type and mutant forms of IA_3 was performed by automated Edman degradation on protein bands that were electroblotted onto polyvinylidene difluoride membrane following SDS-polyacrylamide gel electrophoresis on 20% gels. Samples for amino acid analysis were hydrolyzed for 16 h at 105 °C in 6 M HCl before being loaded onto a Biochrom 20 amino acid analyzer (Amersham Pharmacia Biotech, Cambridge, UK). MALDI-TOF mass spectrometry was carried out using a PE Biosystems Voyager Elite XL instrument incorporating a UV laser and delayed extraction. Samples at ~10 pmol/μl were added to a matrix solution consisting of ferulic acid (55 mg/ml in ethanol containing 0.1% trifluoroacetic acid) in a sample/matrix ratio of 3:1.

Kinetic Measurements and Peptide Cleavage—Inhibition assays were conducted at pH 3.1 and 4.7 as described previously (12, 14) using Lys-Pro-Ile-Glu-Phe*NitroPhe-Arg-Leu (where the asterisk indicates the scissile peptide bond) as substrate for all enzymes except yapsin 1 (15). For this enzyme, the substrate used was ACTH (residues 1–39). This was incubated at 37 °C in 50 mM sodium acetate buffer, pH 5.3, with 10 units of purified yapsin 1 (15) for 30 min in the absence and presence of peptide 1 at final concentrations up to 20 μM. The proteolytic product from ACTH (residues 1–15) was detected and quantified by reverse phase high performance liquid chromatography.

The susceptibility of peptide/protein forms of IA_3 to proteolytic cleavage was examined by incubation at 37 °C for various lengths of time (commonly 16 or 72 h) with the appropriate enzyme in 100 mM sodium formate/acetate buffers at pH 3.1/4.7, respectively, each containing 300 mM NaCl. Each synthetic peptide was incubated initially with proteinase A for 16 h at a molar ratio of 40:1 and, if no cleavage was detected under these circumstances, then the incubation was repeated at a peptide:proteinase ratio of 10:1 for 72 h. Peptide 1 was incubated with nontarget proteinases such as human pepsin at both pH 3 and 5 at a molar ratio of 1,000:1 for only 1 h. Each digest was separated by reverse-phase fast protein liquid chromatography using a Pep-RPC column (Amersham Pharmacia Biotech, Bucks, United Kingdom) and the fractions containing any cleavage products were collected and subjected to acid hydrolysis followed by amino acid analysis. Protein samples were frozen for storage prior to subsequent mixing with the matrix solution for application to a stainless steel target and analysis by MALDI-TOF mass spectrometry.

Crystallography and Molecular Modeling—Crystals of a complex of proteinase A with the K24M mutant protein form of IA_3 (Table I) were grown by vapor diffusion under the conditions described previously for other IA_3-proteinase A complexes (12). The initial solution was prepared at a molar ratio of inhibitor:proteinase of 5:1, and after separation from the excess of inhibitor by gel filtration on Sephadex G-50, was concentrated to 5 mg/ml by ultrafiltration. The mother liquor contained 30% PEG1500, 0.14 M ammonium sulfate in 0.1 M MES buffer, pH 6.0. Data extending to 1.9 Å were collected at 100 K on beamline X9B at NSLS, Brookhaven National Laboratory, Upton, NY, using an ADSC 4K CCD detector. Data were processed with HKL2000 (16). The initial data set consisted of 217,446 reflections that could be scaled with R_{sym} of 8.7% (last shell 34.6%) to yield 41,718 unique measurements. The completeness was 92.8% for the whole data and 75.5% for the final shell. The structure of proteinase A complexed with peptide 1 (12) was used as the initial model with replacement of Lys^{24} by Met. The structure was refined with CNS 1.0 (17) utilizing data extending to 2.0-Å resolution. The first two rounds of refinement included positional and B factor refinements and model adjustment, while solvent molecules were added in the third round. The final model contained the enzyme, residues 2–31 of the inhibitor and 243 water molecules. The final R factor was 19.84% and R_{free} was 23.1%. The root mean square deviations for bond lengths and bond angles from ideality was 0.012 and 1.59 Å, respectively.

Modeling calculations were made on a Silicon Graphics Octane with a single R12000 processor using the Moloc modeling package. Individual amino acid side chains (K18M/D22L) in IA_3 were changed with a built-in function in Moloc. Side chain conformations were adapted manually and a subsequent round of optimization, maintaining proteinase A and the remainder of IA_3 fixed, resulted in low energy conformations for the newly introduced side chains. The new protein-inhibitor complex was checked for attractive and repulsive interactions, and allowed conformations, respectively.

RESULTS AND DISCUSSION

Interaction of Protein/Peptide Forms of IA_3 with Target and Nontarget Enzymes—The nucleotide sequence encoding all 68 residues of IA_3 was amplified by PCR and introduced into the pET-22b vector for expression in *E. coli* as described under "Experimental Procedures." The recombinant protein that accumulated in *E. coli* was soluble and was purified to homogeneity from cell lysates by taking advantage of the His_6 tag introduced from the pET-22b vector at the C terminus of the IA_3 polypeptide chain (see "Experimental Procedures"). N-terminal analysis of one batch of the homogeneous wild-type inhibitor through 10 cycles of Edman degradation gave the sequence Asn-Thr-Asp-Gln-Gln-Lys-Val-Ser-Glu-Ile, which is exactly coincident with that predicted by the DNA sequence for residues 2–11 (Table I) (11) and indicates that the initiator Met^1 residue had been removed during the accumulation of this batch of recombinant protein in *E. coli*. Analysis of a separate batch of recombinant wild-type inhibitor by MALDI-TOF mass spectometry gave a mass of 8772 Da, identical with that predicted (8772 Da) for the IA_3 sequence plus the C-terminal extension of ~Leu-Glu-His_6 introduced from the pET-vector.

The K_i value determined at pH 3.1 for the inhibition of yeast proteinase A by this C-terminal tagged, wild-type recombinant protein (wild-type in Table I) was comparable to that reported previously at the same pH for the naturally occurring protein purified from *S. cerevisiae* (14). It is readily apparent then that the introduction of the extra ~Leu-Glu-His_6 residues at the C terminus of the recombinant inhibitor did not have any significant detrimental effect on inhibitory potency. Since the target proteinase is unlikely ever to encounter a pH as low as 3.1 in its cellular environment, attempts were also made to determine inhibition constants at higher pH values such as 4.7 and 6.0. In both cases, the interaction with proteinase A was so tight that the K_i values lay at or beyond the limits of accurate determination using the available assay methodology and so were estimated to be <0.1 nM.

A synthetic peptide which spanned residues 2–34 of the IA_3 sequence (Peptide 1 in Table II) was found to have inhibitory potency against yeast proteinase A at pH 3.1 and 4.7 compa-

TABLE I

Interactions between yeast proteinase A and protein forms of IA_3

Recombinant protein forms of IA3 consisting of 68 residues plus a ~Leu-Glu-$(His)_6$ tag at their C terminus were produced in *E. coli* and purified to homogeneity. The sequence of residues 2–32 (only) of each protein is given.

Identifier	Sequence	K_i pH 3.1	K_i pH 4.7
	2 5 10 15 20 25 30	nM	
Wild-type	NTD QQKVS EIFQS SKEKL QGDAK VVSDA FKK~	1.1 ± 0.4	<0.1
Chimera	GGH DVPLT NIFQS SKEKL QGDAK VVSDA FKK~	8 ± 1	<0.1
$(Gly)_9$	GGG GGGGG GIFQS SKEKL QGDAK VVSDA FKK~	40 ± 10	1.0 ± 0.7
K7M	NTD QQMVS EIFQS SKEKL QGDAK VVSDA FKK~	2 ± 1	<0.1
K24M	NTD QQKVS EIFQS SKEKL QGDAM VVSDA FKK~	1.3 ± 0.4	<0.1
K31M/K32M	NTD QQKVS EIFQS SKEKL QGDAK VVSDA FMM~	0.9 ± 0.3	<0.1
MIX	NTD QQKVS EIFQS SKEKL QGDAK VVKAD KFS~	800[a]	50 ± 16
D22L	NTD QQKVS EIFQS SKEKL QGLAK VVSDA FKK~	8 ± 2	0.6 ± 0.3
K18M/D22L	NTD QQKVS EIFQS SKEML QGLAK VVSDA FKK~	<0.1	<0.1

[a] IC_{50} value.

TABLE II

Interactions between yeast proteinase A and synthetic peptide forms of IA_3

The entire sequence of each peptide is given in full. Z = L-norleucine.

Identity No.	Sequence	K_i pH 3.1	K_i pH 4.7
	2 5 10 15 20 25 30	nM	
1.	NTD QQKVS EIFQS SKEKL QGDAK VVSDA FKKZA	3 ± 0.6	<0.1
2.	NTD QQKVS EIFQS SKEKL QGDAK VVSDV FKKZA	2 ± 0.6	ND[a]
3.	NTD QQKVS KIFQS SKEKL QGDAK VVSDV FKKZA	3 ± 1	ND
4.	TD QQKVS EIFQS SKEKL QGDAK VVSDA FKKZA	4 ± 1	0.8 ± 0.2
5.	D QQKVS EIFQS SKEKL QGDAK VVSDA FKKZA	8 ± 2	6 ± 1.5
6.	KVS EIFQS SKEKL QGDAK VVSDA FKKZA	85 ± 20	29 ± 8
7.	FQS SKEKL QGDAK VVSDV FKKZA-NH_2	NI[b]	500 ± 120
8.	KEKL QGDAK VVSDA FKKZA	No inhibition	
9.	NTD QQKVS EIFQS SKEKL QGDAK VVSDA FKK	15 ± 4	2 ± 0.4
9-NH_2	NTD QQKVS EIFQS SKEKL QGDAK VVSDA FKK-NH_2	5 ± 0.6	0.8 ± 0.3
10.	NTD QQKVS EIFQS SKEKL QGDAK VVSDA F	25 ± 8	5 ± 1
10-NH_2	NTD QQKVS EIFQS SKEKL QGDAK VVSDA F-NH_2	8 ± 3	2 ± 0.6
11.	NTD QQKVS EIFQS SKEKL QGDAK VVSDA	700 ± 200	400 ± 80
11-NH_2	NTD QQKVS EIFQS SKEKL QGDAK VVSDA-NH_2	240 ± 50	60 ± 9
12.	NTD QQKVS EIFQS SKEKL QGDAK VVSD	NI	1,000 ± 300
13.	NTD QQKVS EIFQS SKEKL QGDAK VV	No inhibition	
14.	NTD QQKVS EIFQS S	No inhibition	

[a] ND, not determined.

[b] NI, no inhibition at a final concentration of 2 μM.

rable to those of the naturally occurring and wild-type recombinant protein forms of IA_3, described previously (12, 14). In contrast, peptide 1, at a concentration of 2 μM, had no significant ability to inhibit any one of a number of other aspartic proteinases from a wide range of other species (Table III). These have considerable sequence and structural similarities to yeast proteinase A and included yapsin 1 (a membrane-attached aspartic proteinase also from *S. cerevisiae* (15) and other enzymes of fungal, mammalian, parasite (plasmepsin II from *Plasmodium falciparum* (18) and plant (cyprosin from *Cynara cardunculus* (19)) origin. Thus, IA_3 is a potent specific inhibitor directed solely against its target enzyme, yeast proteinase A. Since peptide 1 had no effect on the nontarget enzymes listed in Table III, reciprocally, the effect of a number of these (including *e.g.* human pepsin, cathepsin D, and cathepsin E) on peptide 1 was examined. With human pepsin, for example, using a molar ratio of peptide 1:pepsin of 1,000:1 at pH 3.1 and pH 5, peptide 1 was cleaved rapidly at the ~Glu^{10}*Ile^{11}~ and ~Ala^{29}*Phe^{30}~ bonds, as revealed by amino acid analysis of the collected peptide fragments (data not shown). Identical results were obtained for the other enzymes so it would appear that peptide 1 is unable to inhibit the nontarget aspartic proteinases such as pepsin, cathepsins D and E (and the other enzymes listed in Table III) because these enzymes cut the polypeptide effectively as a substrate. Consequently,

TABLE III

Aspartic proteinases unaffected by the IA_3 inhibitor

The activity of each enzyme at the appropriate, indicated pH value was not affected significantly by inclusion of peptide 1 at a final concentration of 2 μM in each assay.

Enzyme	Assay pH	Enzyme	Assay pH
Yapsin 1	5.3	Human pepsin	4.7
Penicillopepsin	4.7	Human gastricsin	4.7
Endothiapepsin	4.7	Human cathepsin D	4.7
Mucor miehei proteinase	4.7	Human cathepsin E	4.7
Mucor pusillus proteinase	4.7	Human napsin	4.7
S. lignicolum proteinase A	4.7	Calf chymosin	4.7
Glomerella cingulata proteinase	4.7	Plasmepsin II	4.4
		Cyprosin	5.0

the ~Ala^{29}*Phe^{30}~ and ~Glu^{10}*Ile^{11}~ sites that were cleaved by the nontarget proteinases were changed singly and in concert to introduce residues at the P_1 position which were known from extensive previous studies (*e.g.* Refs. 20 and 21) to be refractory to cleavage by such enzymes as human pepsin and cathepsin D. The resultant peptides (2 and 3, Table II) were just as potent as peptide 1 as inhibitors of proteinase A but still showed no significant ability to inhibit, *e.g.* human pepsin or cathepsin D at concentrations as high as 5 μM. Although cleavage of peptides 2 and 3 between residues ~Val^{29}-Phe^{30}~ and

~Lys[10]-Ile[11]~ plus ~Val[29]-Phe[30]~, respectively, was no longer evident, nevertheless, cleavage at other locations now became apparent. For example, after incubation of peptide 3 with human cathepsin D at pH 3.1, the digest was analyzed by MALDI-TOF mass spectrometry and the large product that was detected (3238 Da observed; 3237 Da predicted) indicated that cleavage had occurred between residues ~Gln[5]*Gln[6]~ to generate the fragment spanning residues 6–34. Thus, peptides 1, 2, and 3 appeared to be cleaved by the nontarget proteinases including human pepsin and cathepsin D at whatever peptide bonds were accessible and which met the sub-site specificity requirements of each enzyme.

In contrast, peptides 1, 2, and 3 were not cleaved by proteinase A (at pH 3.1 or 4.7), even upon prolonged incubation for 3 days at 37 °C at molar ratios of peptide:proteinase A as low as 5:1. Similarly, the recombinant, wild-type protein form of IA_3 (Table I) was not cleaved by yeast proteinase A since the mass ion (8772 Da) observed by MALDI-TOF mass spectrometry after prolonged incubation was identical to that of the starting material. However, the wild-type protein was digested by pepsin and cathepsin D, *e.g.* analysis of the material incubated at pH 3.1 with human cathepsin D indicated that one large product had accumulated which was consistent in size (5575 Da observed; 5578 predicted) with that of a fragment spanning residues Phe[30]-Glu[68] plus the ~Leu-Glu-$(His)_6$ tag. Thus the full-length protein form of IA_3 also appears to be degraded by nontarget proteinases with cleavage taking place, at least, at one of the bonds (~Ala[29]*Phe[30]~) that was identified earlier for peptide 1 (no attempts were made to detect by mass spectrometry any small products from the N terminus of IA_3 in the cathepsin D digest). This ready susceptibility of IA_3 in both peptide and protein forms to proteolytic cleavage by nontarget enzymes provides further substantiation to our conclusion described previously (12) that the free IA_3 polypeptide has little intrinsic secondary structure.

Truncation and Mutagenesis of IA_3—Since the inhibitory activity of IA_3 toward proteinase A appeared to be contained within residues 2–34 (compare K_i values for the wild-type protein form (Table I) and the peptide form (peptide 1, Table II)), the effect on inhibitory potency of further truncation of this sequence was examined using a systematic series of synthetic peptides in which residues were successively deleted from the N and C termini. Removal of Asn[2] had little effect on the K_i value measured at pH 3.1 (compare peptide 4 with peptide 1, Table II) but the potency was diminished somewhat at pH 4.7, as a K_i value was readily quantified for peptide 4 at this pH value (Table II). Similarly, deletion of residues 3–6 progressively diminished inhibitory potency (peptides 5 and 6, Table II) and the absence of residues 2–11 (in peptide 7) resulted in almost complete abolition of the inhibitory activity. The activity of IA_3 was totally destroyed when residues 2–15 were lacking (peptide 8, Table II). The residues at the N-terminal end of the 2–34 polypeptide sequence would thus appear to contribute substantially to the potency of inhibition.

To investigate the importance of the individual side chains of these residues, alterations in sequence were introduced into the full-length protein form of IA_3 at its N terminus by PCR mutagenesis as described under "Experimental Procedures." Initially, residues 2–10 of the wild-type IA_3 sequence were replaced with Gly-Gly-His-Asp-Val-Pro-Leu-Thr-Asn. This is the sequence of residues that is present at the N terminus of the target enzyme, yeast proteinase A itself (22) and, as such, was chosen totally arbitrarily. The recombinant, chimera inhibitor was purified to homogeneity and 10 cycles of Edman degradation yielded the sequence Gly-Gly-His-Asp-Val-Pro-Leu-Thr-Asn-Ile, identical to that predicted by the DNA sequence, and indicating once again that the initiator Met[1] residue had been removed by *E. coli* proteinases. Consistent with this, analysis by MALDI-TOF mass spectrometry gave a mass of 8502 Da, identical to that (8502 Da) predicted for the sequence of residues 2–68 plus the ~Leu-Glu-His_6 tag of the chimeric protein. Remarkably, this chimeric protein with 9/34 (26%) of its residues exchanged was still almost as effective as an inhibitor as the wild-type protein, with its interaction at pH 4.7 still being so tight as to lie at or beyond the limits of accurate determination (Table I). This result, together with the deletion experiments described above with the peptide form of IA_3, suggests that, for effective inhibition, backbone atoms contributed by residues 2–10 are essential but that the (side chain) identity of the individual amino acids in these positions is of lesser importance. On this basis, we replaced residues 2–10 of the natural sequence with nine glycine residues ($(Gly)_9$ mutant, Table I) and purified the resultant protein to homogeneity. No attempts were made to sequence this protein because of the plethora of glycine residues but MALDI-TOF mass spectrometry gave a mass of 8124 Da, identical to that (8124 Da) predicted by the nucleotide sequence but, once again, lacking the initiator Met[1] residue. The yield of this mutant protein obtained from *E. coli* was about 5-fold lower than that obtained for the wild-type (and other mutant) sequence(s). This drastic introduction of nine consecutive glycine residues resulted in a poorer inhibitor with a K_i of 40 nM at pH 3.1 (Table I). However, at pH 4.7, the $(Gly)_9$ mutant protein was still a very effective inhibitor, with its potency quantified at around 1 nM (Table I). Thus, the main chain atoms at the N terminus of the 2–34 sequence would appear to be the major contributors to inhibitory potency from this region with only minor influences being introduced by the individual residue side chains. This was substantiated further by replacement of individual residues, for example, the Lys[7] residue was replaced with methionine which is quasi-isosteric with lysine but lacks the ϵ-NH_2 group. This K7M mutant inhibitor was just as potent as the wild-type protein (Table I).

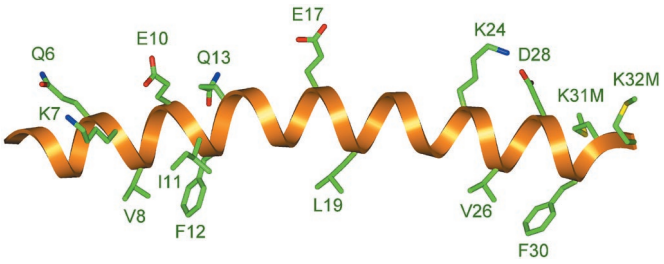

FIG. 1. **The helical conformation adopted by residues 2–32 of IA_3 upon interaction with the active site of proteinase A.** The sequence shown is that of the K31M/K32M mutant, depicting the distribution of selected hydrophilic and hydrophobic residues on opposite faces of the amphipathic helix.

Truncation of the inhibitory sequence of residues 2–34 at its C terminus also resulted in a progressive loss of inhibitory potency (compare peptide 1 and peptides 9, 10, 11, 12, and 13, Table II). Replacement of Lys[24] by Met (K24M mutant) and Lys[31] + Lys[32] (together) in the double mutant K31M/K32M again had no significant effect on the inhibitory potency of the resultant inhibitors toward proteinase A (Table I). The structure of the K24M mutant complexed with proteinase A was solved at 2-Å resolution and refined to an R factor of 19.84% (see "Experimental Procedures"). Comparison with the structures reported previously (12) for the K31M/K32M protein form and for the peptide 1 form of IA_3 complexed with proteinase A (Protein Data Bank accession codes 1dp5 and 1dpj) revealed that, in all three cases, residues 2–32 of the inhibitor had adopted a near-perfect α−helical conformation in the active

TABLE IV

Interactions between yeast proteinase A and synthetic peptide forms of IA_3

The entire sequence of each peptide is given in full.

Identity No.	Sequence	K_i pH 3.1	K_i pH 4.7
	2 5 10 15 20 25 30	*nM*	
9.	NTD QQKVS EIFQS SKEKL QGDAK VVSDA FKK	15 ± 4	2 ± 0.4
15.	NTD QQKAS EIFQS SKEKL QGDAK VVSDA FKK	70 ± 15	8 ± 2
16.	NTD QQKVS EAFQS SKEKL QGDAK VVSDA FKK	60 ± 25	7 ± 2
17.	NTD QQKVS EIAQS SKEKL QGDAK VVSDA FKK	400 ± 40	55 ± 11
18.	NTD QQKAS EIAQS SKEKL QGDAK VVSDA FKK	2,100 ± 300	330 ± 80
19.	NTD QQKVS EAAQS SKEKL QGDAK VVSDA FKK	NI[a]	800 ± 200
20.	NTD QQKAS EAAQS SKEKL QGDAK VVSDA FKK	No inhibition	
10.	NTD QQKVS EIFQS SKEKL QGDAK VVSDA F	25 ± 8	5 ± 1
21.	NTD QQKVS EIFQS SKEKL QGDAK VVSDA A	175 ± 60	35 ± 6
22.	NTD QQKVS EIFQS SKEKL QGDAK VVSDA G	200 ± 70	75 ± 14
23.	NTD QQKVS EIFQS SKEKL QGDAK VVSDA K	200 ± 90	76 ± 9
24.	NTD QQKVS EIFQS SKEKL QGDAK VASDA F	10 ± 2	6 ± 1
25.	NTD QQKVS EIFQS SKEKL QGDAK VDSDA F	150 ± 55	400 ± 130
26.	NTD QQKVS EIFQS SKEKL QGDAK VDSDA K	No inhibition	
27.	NTD QQKVS EIFQS SKEKA QGDAK VVSDA FKK	NI	700 ± 120

[a] NI, no inhibition at a final concentration of 2 μM.

site cleft of the enzyme. Electron density was only observed for these residues in all 3 structures and the root mean square deviation between the Cα coordinates was 0.224 between the protein and peptide form(s) of the inhibitor. The IA_3 helix is amphipathic with the charged residues including Lys^{24} located on one face, protruding into solvent (Fig. 1).

The structures all reveal that the main chain carbonyl and amido moieties of residues 2–10 of the IA_3 polypeptide are involved in H-bond formation with one another within the helix of the inhibitor but the side chains of these residues make no significant contacts with the proteinase, with the exception of Val^8 which is involved in hydrophobic interactions (described later). In the sequence of the chimera inhibitor described earlier (Table I), Val^8 was replaced with Leu which may be able to make hydrophobic contacts with the enzyme requiring only minor re-adjustment so that the derived K_i value was not significantly perturbed. The binding energy of these contacts is clearly lost in the $(Gly)_9$ mutant protein but since the side chains of all of the other residues in the 2–10 sequence point largely into solvent, the still considerable inhibitory potency of the $(Gly)_9$ mutant (Table I) can be readily understood. The predominant requirement in this N-terminal region appears to be for the backbone atoms to satisfy the H-bonding arrangement within the inhibitory helix, thereby stabilizing the helix by providing a somewhat lengthy "cap."

A comparable extended "capping" arrangement exists at the C-terminal end to stabilize the inhibitory helix. No electron density was observed for the side chains of any residues beyond Lys^{32} in the crystal structure of the K24M mutant complex or in the structure of peptide 1 complexed with proteinase A described previously (12) and the side chain of residue 32 makes no significant contacts with the enzyme. Yet the most potent inhibition (subnanomolar at pH 4.7) was measured when the IA_3 sequence was extended at its C terminus beyond Lys^{32}. This was achieved by the inclusion of Nle^{33} (a synthetic isostere of the natural Met residue at this location) and Ala^{34} in peptide 1 (Table II) or by introducing a C-terminal Lys^{32} amide (peptide 9-NH_2, Table II) to stabilize the part of the inhibitor helix necessary for interaction with the proteinase by dissipation of the negative charge from the macromolecular dipole. The contribution of the main chain amido groups in satisfying the H-bonding arrangements at this end of the helix is substantiated by the increased potencies that were measured when each peptide terminated in a C-terminal amide instead of the free COOH group (compare peptides 9-NH_2, 10-NH_2 and 11-NH_2 with 9, 10, and 11, respectively, Table I). A peptide that consisted only of residues 2–28 had lost essentially all of its inhibitory potency (peptide 12, Table II) and residues 2–26 (peptide 13) were not active at all as an inhibitor.

Hydrophobic Clusters—Peptide 14 and peptide 8 (Table II) together span the entire sequence of residues 2–34. Neither of these "half-sized" peptides was able to inhibit proteinase A when added singly or in combination with each other at a variety of molar ratios. Thus a contiguous sequence is necessary for IA_3 to inhibit proteinase A by forming the amphipathic helix (Fig. 1). The residues located on the hydrophobic face make extensive hydrophobic contacts with cognate residues in proteinase A. Particularly noticeable in this regard (Fig. 1) is the "cluster" arrangement of Val^8-*X*-*X*-hydrophobic-Phe^{12} toward the front end of the helix and Val^{26}-*X*-*X*-hydrophobic-Phe^{30} at the back end of the inhibitory sequence. In the front end cluster, replacement of Val^8 or Ile^{11} individually by Ala had minor effects on inhibitory potency (compare peptides 15 and 16 with peptide 9, Table IV). However, deletion of the benzene ring of phenylalanine at position 12 resulted in a considerably larger drop in potency in the resultant Ala-containing peptide (peptide 17, Table IV), emphasizing the importance of van der Waals interactions of this benzene ring with its hydrophobic environment (Fig. 2). The peptide carrying the double replacement of V8A together with F12A (peptide 18, Table IV) had lost much of its inhibitory potency and the double mutant peptide containing ~Ala^{11}-Ala^{12}~ (peptide 19) was virtually ineffective as an inhibitor, even at pH 4.7. The triple mutant in which all three of the front-end cluster residues were changed to ~Ala^8-*X*-*X*-Ala^{11}-Ala^{12}~ (peptide 20, Table IV) was completely inactive as an inhibitor.

A similar response was quantified when the residues contributing to the ~Val^{26}-*X*-*X*-hydrophobic-Phe^{30}~ cluster at the back end of the helix were replaced. Substitution of Phe^{30} by Ala, Gly, or Lys (compare peptides 21 and 22/23 with peptide 10, Table IV) resulted in a significant loss in potency, again emphasizing the contribution to binding by appropriate positioning of the large benzene ring of the side chain of Phe^{30}. In contrast, replacement of Val^{26} by Ala did not diminish inhibitory potency. Rather, it appeared to improve the binding interaction at pH 3.1 marginally (peptide 24, Table IV). Replacement of the -CH_3 side chain of Ala with the -CH_2-COOH side chain of an Asp at position 26 diminished the inhibitory potency at pH 4.7 by about 70-fold (compare peptides 25 and 24, Table IV), commensurate with the introduction of a hydrophilic

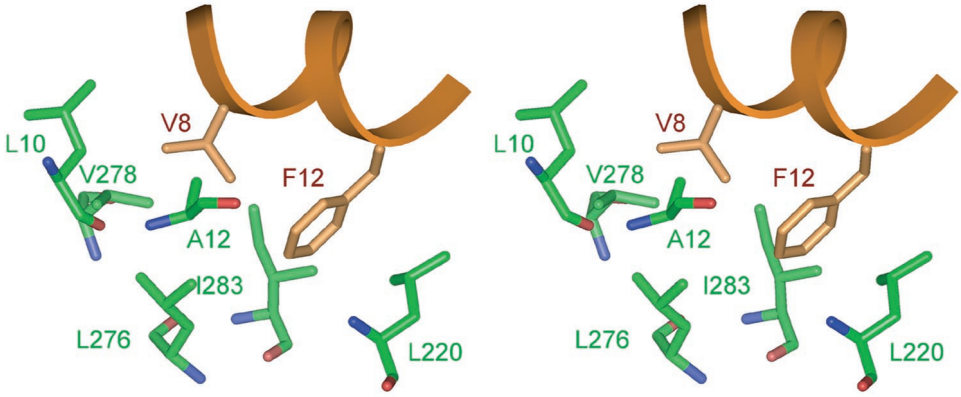

FIG. 2. **Stereo representation of the interactions made by the side chains of Val^8 and Phe^{12} in the IA$_3$ polypeptide with cognate hydrophobic residues in proteinase A.** Proteinase A residues are *green* while the Val^8 and Phe^{12} side chains and the appropriate segment of the IA$_3$ helical backbone are in *brown*.

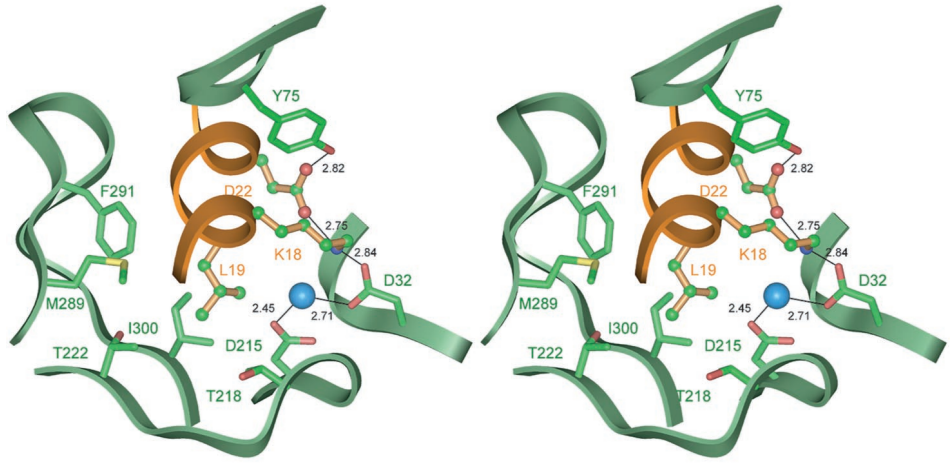

FIG. 3. **Stereo representation of the interactions made by the ~Lys^{18}-Leu^{19}-*X*-*X*-Asp^{22}~ centerpiece residues of IA$_3$ in the vicinity of the active site of proteinase A.** Proteinase A residues are in *green* with the catalytic water molecule depicted as a *blue sphere*. The side chains of Lys^{18}, Leu^{19}, and Asp^{22} plus the relevant segment of the IA$_3$ helix backbone are in *brown*. Hydrogen bonding distances are shown.

side chain into a hydrophobic environment. However, the K_i value measured at pH 3.1 for peptide 25 was tighter than that derived at pH 4.7 (Table IV). Of all the inhibitors listed in Tables I, II, and IV, this was the only occasion when such an effect was observed and most likely is a reflection of the Asp side chain in its protonated and therefore uncharged form being less unfavorable in its contact with the hydrophobic environment offered by the enzyme.

The double mutant peptide carrying the V26D/F30K substitutions was completely ineffective as an inhibitor (peptide 26, Table IV), indicating that introduction of two hydrophilic, charged residues was highly unfavorable since there are no H-bond partners available in the enzyme to compensate for desolvation of the two side chain functions. However, amphipathic helices are often stabilized by electrostatic interactions between residues at positions i and $i + 4$ (23) and, indeed exactly such a salt bridge is present between the Lys^{24} and Asp^{28} residues on the hydrophilic face of the IA$_3$ helix when complexed with its target proteinase (Fig. 1). However, the attempt to encourage Asp^{26} and Lys^{30} to interact with one another to form an additional salt bridge in the V26D/F30K double mutant peptide was clearly not tolerated on the hydrophobic face of the amphipathic helix in the active site cleft of the enzyme. A further mutant was also constructed in which the sequence of ~Ser^{27}-Asp^{28}-Ala^{29}-Phe^{30}-Lys^{31}-Lys^{32}~ was shuffled to ~Lys^{27}-Ala^{28}-Asp^{29}-Lys^{30}-Phe^{31}-Ser^{32}~ in the protein form of the IA3 inhibitor (Mix in Table I). In this arrangement, Val^{26} was retained but the salt bridge between Lys^{24} and Asp^{28} on the hydrophilic face of the helix was disrupted and the crucial Phe^{30} residue was replaced by lysine, as in peptide 23. The resultant mutant protein (Mix, in Table I) was purified to homogeneity from *E. coli* and found to have a K_i value at pH 4.7 comparable to that observed for the single F30K mutant peptide (peptide 23, Table IV). This might be interpreted to indicate that the salt bridge interaction between Lys^{24} and Asp^{28} on the hydrophilic surface of the IA$_3$ helix is, not unexpectedly, weak.

Central Residues in the Inhibitor Helix—The "centerpiece" of the inhibitory 2–34 residues of IA$_3$ is the ~Lys^{18}-Leu^{19}-*X*-*X*-Asp^{22}~ sequence. In the three crystal structures of the K24M and K31M/K32M mutant proteins and peptide 1 forms of IA3 complexed with proteinase A, the ϵ-NH$_2$ group of Lys^{18} of the inhibitor hydrogen bonds to one of the carboxyl oxygens of Asp^{32} of the enzyme (Fig. 3). This is one of the two catalytic Asp residues that operate the catalytic mechanism of all aspartic proteinases (24). The ϵ-NH$_2$ group of Lys^{18} also hydrogen bonds to one of the carboxyl oxygens of the side chain of Asp^{22} in the IA$_3$ inhibitory sequence (Fig. 3). The other oxygen of the side chain COOH of Asp^{22} hydrogen bonds to the phenolic OH group of Tyr^{75} in the enzyme, a residue that is totally conserved in all eukaryotic aspartic proteinases and which is positioned almost at the tip of the β-hairpin loop or flap that overlays the active site cleft in these enzymes. A network of interactions thus cross-links these charged residues of IA$_3$ with the catalytically

essential and structurally conserved residues of the target enzyme (Fig. 3). When the charged side chain of Asp^{22} in the full-length protein form of IA_3 was replaced with the hydrophobic but otherwise almost isosteric side chain of a leucine residue, the purified D22L mutant protein had a slightly reduced potency both at pH 3.1 and 4.7 (Table I) but nevertheless was still an effective inhibitor.

However, when Lys^{18} was changed to Met in concert with the D22L mutation, the resultant inhibitor (K18M/D22L, Table I) was an extremely *potent* inhibitor. For the first time in all of these studies, it was not possible to derive an accurate K_i value at pH 3.1 because the protein-protein interaction was so tight. This may be a reflection of the increased propensity of Met and Leu residues to be accommodated within a helical conformation by comparison with their wild-type Lys and Asp counterparts. Alternatively, this may be a further indication of the importance of hydrophobic contributions to binding strength. Modeling studies suggest that the side chain of a methionine at position 18 in the IA_3 sequence is surrounded by the hydrophobic side chains of Ile^{30}, Tyr^{75}, Thr^{111}, Phe^{112}, Phe^{117}, and Ile^{120} of proteinase A, as well as the newly introduced side chain of Leu^{22} in the K18M/D22L double mutant inhibitor. The side chain of Leu^{22} can make potential, favorable interactions with C-β of Ser^{35} and the side chains of Ile^{73} and Tyr^{75} from the flap of proteinase A, as well as with the Met^{18} and Val^{25} residues of the IA_3 inhibitory sequence.

The importance of hydrophobic interactions was further corroborated when the Leu^{19} residue within the ~Lys^{18}-Leu^{19}-*X*-*X*-Asp^{22}~ centerpiece was changed to Ala in the peptide form of IA_3. The resultant peptide (peptide 27, Table IV) was no longer an inhibitor at pH 3.1 and an apparent inhibition constant of 700 nM was estimated at pH 4.7. This loss in potency (compare peptides 27 and 9, Table IV) was the largest observed for any single amino acid replacement. However, when peptide 27 was incubated with proteinase A for 16 h at pH 4.7 and 37 °C at a molar ratio of 40:1, it was cleaved as a substrate (as monitored by reverse phase fast protein liquid chromatography, not shown). Peptide 27 is thus a good alternative substrate at pH 4.7 and was giving only an apparent inhibition of the activity of proteinase A toward the chromogenic substrate used in the inhibition assays. The deletion of the terminal isopropyl moiety of the leucine side chain thus converted a highly potent polypeptide inhibitor into a regular substrate of proteinase A by decreasing affinity to the target enzyme and possibly by reducing internal helix stability.

Under the same conditions, peptides 14 and 8 (Table II) which together span the 2–34 sequence of IA_3 were both cleaved by proteinase A (at the ~Glu^{10}*Ile^{11}~ and ~Ala^{29}*Phe^{30}~ bonds, respectively) as reported previously (12). Peptide 7, despite having been synthesized deliberately to position a valine in place of the natural Ala^{29} residue (Table II) and thus make the potentially vulnerable ~Ala^{29}*Phe^{30}~ peptide bond resistant to attack (as in peptides 2 and 3, see earlier), was still cleaved albeit very slowly (50% in 16 h) upon incubation at pH 4.7 with proteinase A at a molar ratio of 40:1. Since cleavage at the mutated ~Val^{29}–Phe^{30}~ bond was no longer an option, it was found by amino acid analysis that processing had taken place at the adjacent ~Phe^{30}*Lys^{31}~ bond (data not shown). Similarly, peptides 12 and 13 (Table II) were digested after 72 h incubation with proteinase A at a molar ratio of 10:1, as were peptides 18, 19, 20, and 26 of the peptides listed in Table IV. Thus, in addition to the L19A mutant (peptide 27) as described above, the other peptides (7, 8, 12, 13, 14 (Table II), 18, 19, 20, and 26 (Table IV)) which were not effective as inhibitors of proteinase A, served instead as substrates for the enzyme.

From all of these data, it is readily apparent that the inhibitory capacity of IA_3 is located within residues 2–34 of the sequence and that these residues need to be present as a contiguous polypeptide to achieve inhibition. The inhibitory sequence of residues is not cleaved by the target enzyme but only very subtle alterations in sequence are necessary to convert the IA_3 polypeptide into a substrate for proteinase A. In contrast, however, the wild-type polypeptide is readily hydrolyzed as a substrate by nontarget aspartic proteinases such as pepsin and cathepsin D, which have substantial similarity to proteinase A in their primary sequences and three-dimensional structures (25–27). This substantiates our NMR and CD findings reported previously (12) that free IA_3 in its peptide or protein forms is predominantly unstructured. The interaction of IA_3 with its target enzyme appears to depend critically on the insertion of three hydrophobic "pins" (the front-end cluster, Leu^{19} and the back end cluster) into the appropriate hydrophobic sockets proferred by the active site cleft of proteinase A. The target enzyme thus plays the role of a helper template, stabilizing the amphipathic helical conformation of IA_3 but, paradoxically, resulting in its own inhibition. In contrast, the random coil IA_3 polypeptide is apparently unable to locate the critical pins sufficiently precisely in its interaction with the nontarget aspartic proteinases. Consequently, since aspartic proteinases generally require only 7 or 8 amino acid residues of a polypeptide to bind in an extended β-strand conformation in their active site to act as a substrate, the nontarget enzymes are readily able to cleave IA_3. Thus, the "default" setting is cleavage of the random coil IA_3 polypeptide. In contrast, helication requires many more stringent conditions to be fulfilled such as complementary amphipathicity, precision of shape, and the correct juxtaposition of side chains possessing the appropriate properties to fit snugly into the hydrophobic pockets of proteinase A. Only if IA_3 can be sculpted *in situ* to become the key that matches precisely into the lock that is the active site of proteinase A, can the IA_3 polypeptide escape cleavage and preserve its integrity. Thus, in its interaction with this aspartic proteinase, IA_3 is stabilized in the somewhat abnormal helical conformation, shaped by the proteinase itself but yet at the same time, held clear of the catalytic machinery through formation of the helix. The alternative, as a consequence of any imprecision of fit, is recognition in an extended conformation and cleavage.

The present study has thus afforded considerable insight into the features that are important in governing the potency and selectivity of inhibition of proteinase A by IA_3. This presents a fascinating challenge for future investigation to determine whether this unprecedented mode of inhibitor-enzyme interaction can be exploited to generate selective inhibitors re-targeted against other aspartic proteinases including those produced by pathogenic organisms.

Acknowledgments—It is a pleasure to acknowledge the valuable contributions made to this project by our colleagues Anette Bruun (Carlsberg Laboratory), Alfred Chung (Protein Chemistry Core, University of Florida), Simon Cater (Cardiff School of Biosciences), and Jerry Alexandratos (NCI-Frederick). We are also very grateful to Professor Pat Sullivan and Drs. Peter Farley and William Laing, New Zealand, for generously providing the proteinase from *Glomerella cingulata*; Drs Niamh Cawley and Y. Peng Loh, National Institutes of Health, Bethesda, MD, who very kindly performed the inhibition experiments with peptide 1 on yapsin 1; and Professor Simon Gaskell, Center for Mass Spectrometry, UMIST, UK, for providing ready access to mass spectrometer facilities.

REFERENCES

1. Vassar, R., Bennett, B. D., Babu-Khan, S., Kahn, S., Mendiaz, E. A., Denis, P., Teplow, D. B., Ross, S., Amarante, P., Loeloff, R., Luo, Y., Fisher, S., Fuller, J., Edenson, S., Lile, J., Jaronsinski, M. A., Biere, A. L., Curran, E., Burgess, T., Louis, J-C., Collins, F., Treanor, J., Rogers, G., and Citron, M. (1999) *Science* **286,** 735–741

2. Bennett, B. D., Babu-Khan, S., Loeloff, R., Louis, J-C., Curran, E., Citron, M., and Vassar, R. (2000) *J. Biol. Chem.* **275,** 20647–20651
3. Kay, J., Valler, M. J., and Dunn, B. M. (1983) in *Proteinase Inhibitors Medical and Biological Aspects* (Katunuma, N., Umezawa, H., and Holzer, H., eds) pp. 201–210, Japan Scientific Societies Press, Tokyo
4. Takahashi, S., Takahashi, K., Kaneko, T., Ogasawara, H., Shindo, S., and Kobayashi, M. (1999) *J. Biochem.* (*Tokyo*) **125,** 348–353
5. Kageyama, T. (1998) *Eur. J. Biochem.* **253,** 804–809
6. Kreft, S., Ravnikar, M., Mesko, P., Pungercar, J., Umek, A., Kregar, I., and Strukelj, B. (1997) *Phytochemistry* **44,** 1001–1006
7. Christeller, J. T., Farley, P. C., Ramsey, R. J., Sullivan, P. A., and Laing, W. A. (1998) *Eur. J. Biochem.* **254,** 160–167
8. Lenarčič, B., and Turk, V. (1999) *J. Biol. Chem.* **274,** 563–566
9. Saheki, T., Matsuda, Y., and Holzer, H. (1974) *Eur. J. Biochem.* **47,** 325–327
10. Biedermann, K., Montali, U., Martin, B., Svendsen, I. B., and Ottesen, M. (1980) *Carlsberg Res. Commun.* **45,** 225–235
11. Schu, P., and Wolf, D. H. (1991) *FEBS Lett.* **283,** 78–84
12. Li, M., Phylip, L. H., Lees, W. E., Winther, J. R., Dunn, B. M., Wlodawer, A., Kay, J., and Gustchina, A. (2000) *Nat. Struct. Biol.* **7,** 113–117
13. Tigue, N. J., and Kay, J. (1998) *J. Biol. Chem.* **273,** 26441–26446
14. Dreyer, T., Valler, M. J., Kay, J., Charlton, P., and Dunn, B. M. (1985) *Biochem. J.* **231,** 777–779
15. Azaryan, A. V., Wong, M., Friedman, T. C., Cawley, N. X., Estivariz, F. E., Chen, H. C., and Loh, Y. P. (1975) (1993) *J. Biol. Chem.* **268,** 11968–11971
16. Otwinowski, Z., and Minor, W. (1997) *Methods Enzymol.* **276,** 307–326
17. Brünger, A. T., Adams, P. D., Clore, G. M., DeLano, W. L., Gros, P., Grosse-Kunstleve, R. W., Jiang, J. S., Kuszewski, J., Nilges, M., Pannu, N. S., Read, R. J., Rice, L. M., Simonson, T., and Warren, G. L. (1998) *Acta Crystallogr. Sect. D* **54,** 905–921
18. Hill, J., Tyas, L., Phylip, L. H., Kay, J., Dunn, B. M., and Berry, C. (1994) *FEBS Lett.* **352,** 155–158
19. White, P. C., Cordeiro, M. C., Arnold, D., Brodelius, P. E., and Kay, J. (1999) *J. Biol. Chem.* **274,** 16685–16693
20. Shintani, T., Nomura, K., and Ichishima, E. (1997) *J. Biol. Chem.* **272,** 18855–18861
21. Arnold, D., Keilholz, W., Schild, H., Dumrese, T., Stevanovic, S., and Rammensee, H. G. (1997) *Eur. J. Biochem.* **249,** 171–179
22. Dreyer, T., Halkier, B., Svendsen, I., and Ottesen, M. (1986) *Carlsberg Res. Commun.* **51,** 27–41
23. Houston, M. E., Kondejewski, L. H., Karunaratne, D. N., Gough, M., Fidai, S., Hodges, R. S., and Hancock, R. E. W. (1998) *J. Peptide Res.* **52,** 81–88
24. Khan, A. R., and James, M. N. G. (1998) *Protein Sci.* **7,** 815–836
25. Sielecki, A. R., Fedorov, A. A., Boodhoo, A., Andreva, N. S., and James, M. N. G. (1990) *J. Mol. Biol.* **214,** 143–170
26. Baldwin, E. T., Bhat, T. N., Gulnik, S., Hosur, M. V., Sowder, R. C., Cachau, R. E., Collins, J., Silva, A. M., and Erickson, J. W. (1993) *Proc. Natl. Acad. Sci. U. S. A.* **90,** 6796–6800
27. Aguilar, C. F., Cronin, N. B., Badasso, M., Dreyer, T., Newman, M. P., Cooper, J. B., Hoover, D. J., Wood, S. P., Johnson, M. S., and Blundell, T. L. (1997) *J. Mol. Biol.* **267,** 899–915